Songklanakarin J. Sci. Technol.
45 (2), 284–293, Mar. – Apr. 2023

http://www.sjst.psu.ac.th

Original Article

Multiple slip effects on dissipative and chemical reactive MHD flows over a permeable stretching sheet in the presence of heat source

Bharat Keshari Swain*

Agarpara College, Agarpara, Bhadrak, Odisha, 756115 India

Received: 7 October 2022; Revised: 21 December 2022; Accepted: 9 March 2023

Abstract

The present investigation construes an unsteady MHD flow over a permeable stretching sheet embedded in a porous medium. The effects of viscous and Darcy dissipation, heat source and chemical reaction have been delineated with the existence of multiple slips. Similarity variables are employed for remodeling the governing equations as a system of first order nonlinear ordinary differential equations. The reduced system is numerically solved with 4^{th} order Runge-Kutta method along with shooting technique. The present results have been verified against earlier works and good agreement was found. The important findings reported herein are: porosity acts as aiding factor for the fluid velocity, more dissipative heat leads to higher velocity and temperature, and chemical reaction parameter adversely affects the concentration. This analysis is relevant to various industrial processes at boundaries of pipes, walls, and/or curved surfaces.

Keywords: viscous dissipation, Darcy dissipation, heat source, chemical reaction, multiple slips

1. Introduction

Magnetohydrodynamics (MHD) may be described as the microscopic interaction of electrically conducting fluid and magnetic field. Its applications range from industries to space science as well as to magnetic therapy. In recent years, MHD flow with the slip condition has received engineering interest. If the viscous force between liquid molecules at the interface is stronger than the force between the molecules of the liquid and molecules of the solid, then the fluid molecules can slide on the solid surface. The resemblance to the mean free path of particles with the flow field characteristic gives rise to the breakdown of Navier-Stokes equations because the hypothesis of continuum media fails. If the Knudsen number (Kn) remains in $1< Kn < 10$, a higher order continuum equation like Burnett equation is appropriate. No-slip condition can't be used (Hak, 1999) in the range of $0.1 > Kn >0.001$. For $Kn < 0.001$, the no-slip condition is appropriate. Particularly, in the case of emulsions, suspensions, etc., no-slip condition is insufficient and slip could occur at the boundary.

*Corresponding author
Email address: bharatkeshari1@gmail.com

The nature of fluid flow under slip condition deviates from that of a standard flow. The slip flows under various configurations were inspected by several researchers. Raza, Rohni, Omar and Awais (2016) illuminated the performance of slip in a nanofluid flowing in a rotating channel. Turkyilmazoglu (2013) did the mass transfer analysis in a slip flow of fluid. Akbar and Khan (2014) have studied the impact of thermal as well as velocity slips on biviscous fluid flow. Hayat, Awais, and Hendi (2012) and Reddy (2016) elucidated the impact of slip condition on rotating flow between two porous walls and on MHD peristaltic flow, respectively. Mabood & Shateyi (2019) studied radiative MHD unsteady flow with multiple slips. Swain, Biswal, and Dash (2021) have investigated the second order slip and heat source effects on dissipative MHD flow of blood through a permeable capillary in stretching motion. They found that skin friction coefficient at the capillary wall decreases with higher order slip.

Application of an external magnetic field in various MHD flow problems is vital. When this flow is considered trough a porous medium, then the study becomes more alluring. These forms of engineering issues are more relevant to energy extraction, oil exploration and also the physical phenomenon management within the field of aeromechanics. So several investigations have been reported by celebrated

researchers. Sekhar, Reddy, Raju, Ibrahim, and Makinde (2018) illustrated the multiple slips impacts on MHD flow through porous medium. Makinde, Khan, Ahmad, and Khan (2018) studied unsteady hydromagnetic radiating fluid flow past a slippery stretching sheet embedded in a porous medium. Makinde, Khan, and Khan (2016) analyzed the MHD nanofluid flow over a convectively heated permeable vertical plate embedded in a porous medium. Mutuku-Njane, and Makinde (2013) illuminated the ramifications of MHD flow of a nanofluid over a convectively heated vertical porous plate through porous medium. Swain and Senapati (2015) inspected the effect of mass transfer on free convective flow set in a porous medium in the presence of magnetic field. Uddin (2015) has also made his analysis considering magnetic field and a porous medium.

The internal energy in the fluid element is modified by the flow of heat and also the performance of work. The work done consists of the reversible half and dissipated work. we tend to solely take into account the contribution from the mechanically dissipated energy per unit volume (SI unit W/m^3), effort aside the contribution of the entropy flux and also the production of entropy stems from the finite temperature distinction in thermal conductivity (Baehr & Stephan, 2006). Anjali and Ganga (2010) investigated the outcome of dissipation for a nonlinear flow with prescribed heat flux. Ferdows, Chapal, and Afify (2014) expounded the nanofluid flow considering permeable stretching sheet and clearly discussed the result of viscous dissipation. Venkateswarlu, Satya Narayana, and Tarakaramu (2018) investigated the viscous dissipation response on MHD flow over a moving surface with constant heat supply. Hunegnaw and Kishan (2017) elucidated the repercussions of viscous dissipation in an unsteady MHD flow over stretching sheet. Biswal, Swain, Das, and Dash (2022) studied the effect of viscous dissipation in their study of MHD stagnation point flow towards an inclined stretching sheet embedded in a porous medium. Swain, Parida, Kar, and Senapati (2020) investigated viscous dissipation and joule heating effect on MHD flow and heat transfer past a stretching sheet embedded in a porous medium. Parida, Swain, and Senapati (2021) analyzed viscous dissipative MHD nanofluid flow over a stretching sheet embedded in a porous medium.

Chemical reaction is additionally of extended importance in fluid flow at the side of the combined impacts of heat and mass transfer. These kinds of studies have applications in several industrial processes and conjointly in physiological flows. Reaction is called to be homogeneous once it happens uniformly through a given part. Otherwise the reaction is termed heterogeneous. Further, a chemical reaction is of first order if the rate of reaction is directly proportional to the concentration. Possible applications may be found in processes like drying, injury of crops because of state change, water surface evaporation etc. Several researchers have done studies on this subject. Chamber and Young (1958) delineated the consequences of homogeneous first order chemical reactions within the neighborhood of a flat plate. Muthucumaraswamy and Janakiramana (2008) and Swain, Senapati, and Dash (2014) have studied the impact of chemical change in MHD physical boundary layer flow past a vertical plate. Ahmed (2014) and Ahmed and Kalita (2014) resolved numerically the MHD flow issues taking care of chemical reaction. Swain, Senapati, and Dash (2017) have conjointly given their interest on resolving the matter of chemical reaction effects on free convective flow. Swain (2021) has also shown his interest on solving the problem of second order chemical reaction effect on MHD convective flow. He explained the consequences of the second order chemical reaction after solving the pertinent equations by finite difference method.

The above studies and applications show the importance of dissipative and chemical reactive MHD flow in the presence of multiple slips. Fluid flow through porous medium and Darcy dissipation, which stems from the resistance offered by viscosity of the fluid in the porous matrix of saturated porous medium, are analyzed here. This type of flow is very applicable in irrigation and drainage problems, in extraction of particulates from soil, cosmetic and petrochemicals products etc. Further, heat source due to temperature difference, which provides thermal power to heat transfer process, may be present. The above aspects are not considered by Mabood and Shateyi (2019) and Mabood and Das (2016). This research gap motivates the present study.

The novelties of the present study are:

- to study the effects of viscous and Darcy dissipation on MHD flow through porous medium
- to analyze the influence of heat source and chemical reaction
- to analyze the flow with multiple slip conditions
- to discuss the works of Mabood & Shateyi (2019), Mabood & Das (2016), Chamkha, Aly, and Mansour (2010) and Ali (1994) as particular cases.

2. Mathematical Formulation

Present analysis deals with a permeable surface along which the *x*-axis is taken. The *y*-axis is drawn normal to x-axis. The fluid flows over a permeable stretching sheet embedded in a porous medium. The sheet is stretched with velocity $U_w(x,t)=\frac{ax}{1-\lambda t}$ in the direction of x-axis. Magnetic field $B(t)=B_0(1-\lambda t)^{-1/2}$ is applied in transverse direction and B_0 is constant initial magnetic field strength. Figure 1 depicts the present flow system. The induced magnetic field is negligible. T_∞ and C_∞ are taken as the ambient temperature and mass concentration respectively. Since the wall is permeable, multiple slips are analyzed.

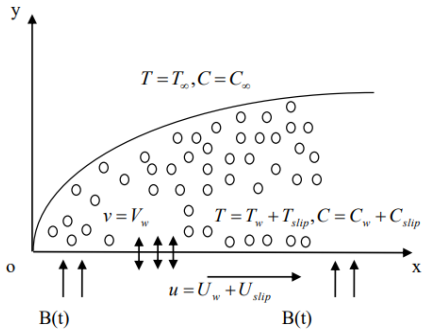

Figure 1. Physical problem

The following points are assumed in the present analysis.

- The two-dimensional viscous flow is unsteady, incompressible, free convective and electrically conducting.
- The stretching permeable sheet is subjected to transverse magnetic field and embedded in porous medium.
- There exist velocity slip, thermal slip as well as solutal slip.
- The induced magnetic field is neglected.
- It is also assumed that no polarization voltage exists.
- The diffusive species is chemically reactive with variable concentration at the surface.

The governing equations are conferred as (cf. Mabood & Shateyi (2019), Misra & Sinha (2013))

$$\frac{\partial u}{\partial x}+\frac{\partial v}{\partial y}=0, \tag{1}$$

$$\frac{\partial u}{\partial t}+u\frac{\partial u}{\partial x}+v\frac{\partial u}{\partial y}=\nu\frac{\partial^2 u}{\partial y^2}-\left(\frac{\sigma B^2(t)}{\rho}+\frac{\nu}{K_p^{*}(t)}\right)u+g\beta_T(T-T_\infty)+g\beta_C(C-C_\infty), \tag{2}$$

$$\frac{\partial T}{\partial t}+u\frac{\partial T}{\partial x}+v\frac{\partial T}{\partial y}=\alpha\left(1+\frac{16T_\infty^{3}\sigma^{*}}{3k^{*}k}\right)\frac{\partial^2 T}{\partial y^2}+\frac{\mu}{\rho C_p}\left(\frac{\partial u}{\partial y}\right)^2+\frac{\mu}{\rho C_p K_p^{*}(t)}u^2+\frac{Q^{*}}{\rho C_p}(T-T_\infty), \tag{3}$$

$$\frac{\partial C}{\partial t}+u\frac{\partial C}{\partial x}+v\frac{\partial C}{\partial y}=D_M\frac{\partial^2 C}{\partial y^2}+D_T\frac{\partial^2 T}{\partial y^2}-R_c^{*}(C-C_\infty) \quad . \tag{4}$$

The boundary conditions are given by

$$\begin{cases} y=0: u=U_w(x,t)+U_{slip}, v=V_w, \\ T=T_w(x,t)+T_{slip}\,,\; C=C_w(x,t)+C_{slip} \\ y\to\infty: u\to 0, T\to T_\infty, C\to C_\infty \end{cases} . \tag{5}$$

Sheet temperature $T_w(x,t)$ and concentration $C_w(x,t)$ at the surface are taken as

$$T_w(x,t)=T_\infty+T_0\left(\frac{ax}{2\nu}\right)(1-\lambda t)^{-2}, C_w(x,t)=C_\infty+C_0\left(\frac{ax}{2\nu}\right)(1-\lambda t)^{-2} \tag{6}$$

where T_0 is the reference temperature and C_0 is the reference concentration and $0\le T_0\le T_W$, $0\le C_0\le C_W$. The above expressions are valid for $(1-\lambda t)>0$.

In equations (2) and (3), $K_p^{*}(t)=k_1(1-\lambda t)$ is the time dependent permeability parameter.

In (5), V_w represents injection/suction velocity of fluid at the surface and is given by

$$V_w=-\sqrt{\frac{a\nu}{1-\lambda t}}f(0).$$

The stream function ψ is expressed as $u=\frac{\partial\psi}{\partial y}$ and $v=-\frac{\partial\psi}{\partial x}$ that satisfy equation (1). The non-dimensional functions and variable f, θ, ϕ and η are taken as follows:

$$\eta=\sqrt{\frac{a}{\nu(1-\lambda t)}}y,\psi=\sqrt{\frac{a\nu}{(1-\lambda t)}}xf(\eta),T=T_\infty+T_0\left(\frac{ax(1-\lambda t)^{-2}}{\nu}\right)\theta(\eta), \tag{7}$$

$$C=C_\infty+C_0\left(\frac{ax(1-\lambda t)^{-2}}{\nu}\right)\phi(\eta)$$

Now putting (7) in equations (2)-(4), the following equations are obtained

$$f''' + ff'' - f'^2 - \delta\left(\frac{\eta}{2} f'' + f'\right) - \left(M + \frac{1}{K_p}\right) f' + \lambda_1\theta + \lambda_2\phi = 0, \tag{8}$$

$$\frac{1}{P_r}(1+R)\theta'' + f\theta' - f'\theta - \delta\left(\frac{\eta}{2}\theta' + 2\theta\right) + E_c f''^2 + D_d f'^2 + Q\theta = 0, \tag{9}$$

$$\phi'' + S_c(f\phi' - f'\phi) - S_c\delta\left(\frac{\eta}{2}\phi' + 2\phi\right) + S_c S_r\theta'' - S_c R_c\phi = 0. \tag{10}$$

The reduced boundary conditions are

$$\begin{aligned} &f(0) = f_w,\ f'(0) = 1 + S_f f''(0), \theta(0) = 1 + S_\theta\theta'(0), \phi(0) = 1 + S_\phi\phi'(0), \\ &f'(\infty) = 0, \theta(\infty) = 0, \phi(\infty) = 0. \end{aligned} \tag{11}$$

The non-dimensional parameters used in (8)-(11) are given by

$$\delta = \frac{\lambda}{a}, \lambda_1 = \frac{g\beta_T T_0}{a\nu}, \lambda_2 = \frac{g\beta_C C_0}{a\nu}, P_r = \frac{\nu}{\alpha}, R = \frac{16T_\infty^{\ 3}\sigma^*}{3k^*k}, M = \frac{\sigma B_0^{\ 2}}{\rho a}, K_p = \frac{ak_1}{\nu}, S_c = \frac{\nu}{D_M}$$

$$S_r = \frac{D_T T_0}{\nu C_0}, f_w = -V_w\sqrt{\frac{1-\lambda t}{\nu a}}, D_d = \frac{E_c}{K_p}, E_c = \frac{U_w^{\ 2}}{C_p(T_w - T_\infty)}, Q = \frac{Q^*(1-\lambda t)}{\rho C_p a}, R_c = \frac{R_c^{\ *}(1-\lambda t)}{a}$$

$$S_f = A_1\sqrt{\frac{a}{\nu(1-\lambda t)}}, S_\theta = A_2\sqrt{\frac{a}{\nu(1-\lambda t)}}, S_\phi = A_3\sqrt{\frac{a}{\nu(1-\lambda t)}}.$$

A_1, A_2, A_3 are velocity slip factor, thermal slip factor and solutal slip factor, respectively.
$A_1 = A_2 = A_3 = 0$ give no-slip conditions.
Here, $f_w = 0$ represents the impermeable surface, $f_w > 0$ produces suction and $f_w < 0$ means injection.
The physical quantities local skin friction coefficient C_f, local Nusselt number Nu and local Sherwood number Sh are defined as

$$C_f = \frac{\mu}{\rho U_w^{\ 2}}\left(\frac{\partial u}{\partial y}\right)_{y=0}, \tag{12}$$

$$Nu = -\frac{x}{k(T_W - T_\infty)}\left[k\left(\frac{\partial T}{\partial y}\right)_{y=0} - \frac{4\sigma^*}{3k^*}\left(\frac{\partial T^4}{\partial y}\right)_{y=0}\right], \tag{13}$$

$$Sh = -\frac{x}{(C_W - C_\infty)}\left(\frac{\partial C}{\partial y}\right)_{y=0}. \tag{14}$$

Putting (7) into equations (12)-(14), the non-dimensional forms obtained are:

$$Cfr = \sqrt{\mathrm{Re}_x}C_f = f''(0), Nur = \frac{Nu}{\sqrt{\mathrm{Re}_x}} = -(1+R)\theta'(0), Shr = \frac{Sh}{\sqrt{\mathrm{Re}_x}} = -\phi'(0), \tag{15}$$

3. Method of Solution

The coupled nonlinear equations (8) - (10) under the boundary conditions (11) have been numerically solved using the fourth order Runge-Kutta method with shooting technique. The equations (8)-(10) have been converted to a set of first order differential equation substituting

$$f = y_1, f' = y_2, f'' = y_3, \theta = y_4, \theta' = y_5, \phi = y_6, \phi' = y_7. \tag{16}$$

The reduced equations are

$$y_3' = -y_1 y_3 + {y_2}^2 + \delta\left(y_2 + \frac{1}{2}\eta y_3\right) + \left(M + \frac{1}{K_p}\right) y_2 - \lambda_1 y_4 - \lambda_2 y_6, \tag{17}$$

$$y_5' = \left(\frac{\Pr}{1+R}\right)\left(-y_1 y_5 + y_4 y_2 + \delta\left(2y_4 + \frac{1}{2}\eta y_5\right) - E_c {y_3}^2 - D_d {y_2}^2 - Q y_4\right), \tag{18}$$

$$y_7' = -S_c\left(y_1 y_7 - y_2 y_6\right) + S_c\delta\left(2y_6 + \frac{\eta}{2} y_7\right) - S_c S_r y_5' + S_c R_c y_6 \tag{19}$$

Boundary conditions are written as

$$y_1 = f_w, y_2 = 1 + S_f y_3, y_3 = ?, y_4 = 1 + S_\theta y_5, y_5 = ?, y_6 = 1 + S_\phi y_7, y_7 = ? \text{ at } \eta = 0, \tag{20}$$

$$y_2 \to 0, y_4 \to 0, y_6 \to 0 \text{ as } \eta \to \infty. \tag{21}$$

For integration, the values of y_3, y_5 and y_7 at $\eta = 0$ are guessed and the step by step integration is accomplished with step length 0.01 adopting shooting technique with MATLAB code having error bound 10^{-3}.

4. Validation

To validate the present results, previous studies are taken into account in Tables 1, 2 and 3. Table 1 and Table 2 give the values of skin friction from previous studies (Chamkha, Aly, & Mansour, 2010; Mabood & Das, 2016; Mabood & Shateyi, 2019) and present results for unsteady parameter and magnetic field parameter respectively. Similarly, some values of Nusselt number of the present study for Prandtl number are compared to the previous studies (Ali, 1994; Mabood & Shateyi, 2019) in Table 3. It is found that the present results are in a good agreement with the earlier studies, which indicates satisfactory accuracy of the present study.

Table 1. $-f''(0)$ for different values of δ when $M = f_w = S_f = \lambda_1 = \lambda_2 = 0$, $K_p \to \infty$

	$-f''(0)$		
Δ	Chamkha, Aly & Mansour (2010)	Mabood and Shateyi (2019)	Present result
0.8	1.261512	1.261042	1.2610428
1.2	1.378052	1.377724	1.3777241

Table 2. $-f''(0)$ for various values of M when $\delta = f_w = S_f = \lambda_1 = \lambda_2 = 0$, $K_p \to \infty$

	$-f''(0)$		
M	Mabood and Das (2016)	Mabood and Shateyi (2019)	Present result
0	−1.000008	−1.0000084	1.0000624
1	1.4142135	1.41421356	1.414213606
5	2.4494897	2.44948974	2.449489744
10	3.3166247	3.31662479	3.316624790
50	7.1414284	7.14142843	7.141428429

Table 3. Values of $-\theta'(0)$ when $M = f_w = S_f = S_\theta = \delta = \lambda_1 = \lambda_2 = R = 0$

	$-\theta'(0)$		
Pr	Ali (1994)	Mabood and Shateyi (2019)	Present result
0.72	0.8058	0.8088	0.809463
1	0.9691	1.0000	1.000062
3	1.9144	1.9237	1.923652
10	3.7006	3.7207	3.720631

5. Results and Discussion

Numerical solutions to an unsteady MHD flow over permeable stretching sheet with multiple slip effects embedded in a porous medium were obtained. The effects of viscous and Darcy dissipation, heat source and chemical reaction are of main concern. The values of pertinent parameters are considered following Mabood and Shateyi (2019) and Mabood and Das (2016). The repercussions of physical parameters are elucidated through graphs and tables assuming the parameters as $P_r = 10$, $S_c = 10$, $\lambda_1 = \lambda_2 = 0.2$, $M = 1$, $S_\theta = S_\phi = S_r = R = 0.5$, $\delta = 0.2$, $f_w = 1$, $S_f = 1$, $E_c = 0.2$, $Q = 0.5$, $K_p = 1$, $K_p = 1$, $R_c = 0.5$ unless otherwise stated.

Figure 2 illustrates the effect of heat source parameter Q on velocity. Increasing Q tends to increase the velocity. Again, this displays the effect of no-slip and first order velocity slip on velocity distribution. It is observed that a decrease in velocity is commensurate with the order of slip. This can be attributed to low momentum transport/diffusion within the boundary layer.

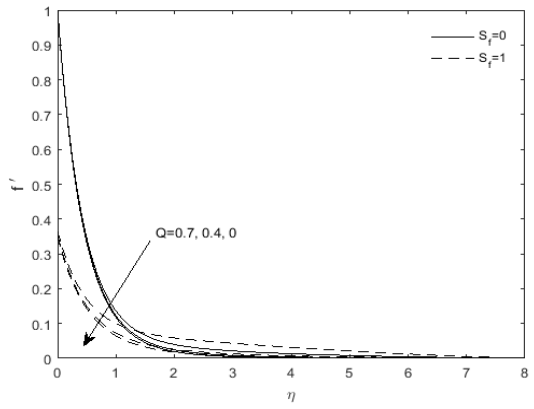

Figure 2. Velocity profile for Q

In Figure 3, porosity parameter K_p acts as contributing to the fluid velocity, i.e. the velocity tends to increase with it. This is because with a rise in permeability of the medium, the regime becomes more porous. As a consequence, the Darcian body force decreases in magnitude (as it is increasing proportional to the permeability). The Darcian resistance acts to decelerate the fluid. This resistance diminishes as permeability of the medium increases. So progressively less drag is experienced by the flow and flow retardation is thereby decreased. Hence, the velocity of the fluid increases as the permeability increases. On careful observation, again it is found that when K_p is increased from 0.1 to 1, rate of change in velocity is higher and after that the rate of increase slows down in the range of K_p from 1 to 10. Again, it is found that velocity slip leads a lower velocity.

Figure 4 elucidates the impacts of Eckert number (E_c) on velocity distribution. The parameter is directly proportional to the velocity. As the Eckert number comes from kinetic energy of flow and heat enthalpy difference, Eckert number correlates positively with the kinetic energy. Again, it is known that temperature represents the average kinetic energy. Viscous dissipative heat tends to raise the temperature. Thus we can say that temperature of the fluid rises. From Figure 6, it is analyzed that fluid temperature rises

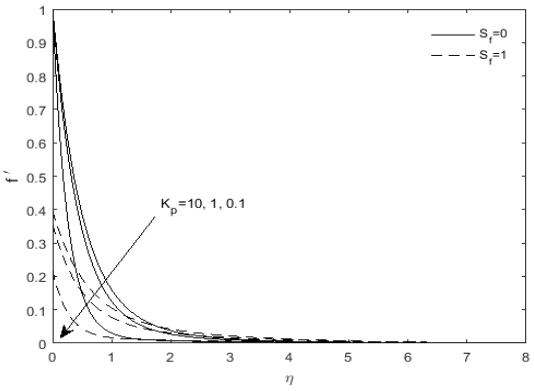

Figure 3. Velocity profile for K_p

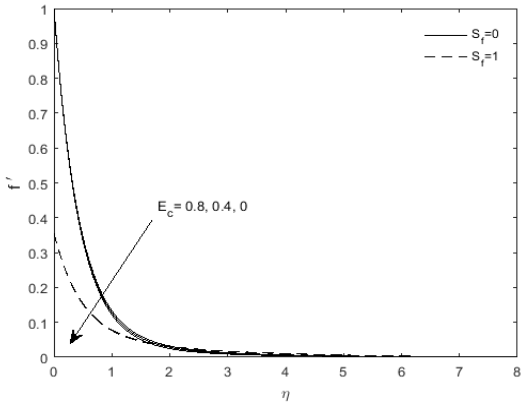

Figure 4. Velocity profile for E_c

as E_c is increased. Due to the higher temperature, resistive power to the fluid flow reduces and the fluid moves with a higher velocity (in Figure 6) for higher values of E_c.

In Figure 5, temperature profiles are drawn for various values of porosity parameter K_p. Increase in both the parameters helps to decrease temperature significantly with and without thermal slip. In case of no thermal slip ($S_\theta = 0$), temperature is comparatively higher.

As heat supply is increased, temperature rises across the flow field in Figure 7. Consequently, it yields a thicker thermal boundary layer. It is pertinent to notice that Q measures internal thermal power per unit volume of the fluid. An increase in heat source means an increase in thermal power. It also gives rise to a lower temperature for first order thermal slip as compared to no-slip condition. Moreover, with increase in temperature the fluid gets thinner and becomes less viscous. Therefore, the fluid flows with higher velocity.

Figure 8 delineates the impact of chemical reaction parameter (R_c) on concentration profile. It is observed that larger values of chemical reaction parameter lead to lower concentration. This is due to the fact that destructive chemical reduces the solutal boundary layer thickness and increases the mass transfer. From a physical point of view, chemical reaction for destructive case is very large. Because of this fact molecular motion is quite high which enhances the transport, thus suppressing the concentration in the fluid. This figure also confirms that a decrease in concentration is commensurate with the order of solutal slip.

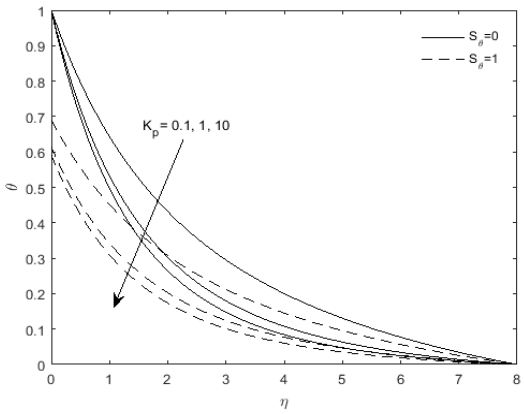

Figure 5. Temperature profile for K_p

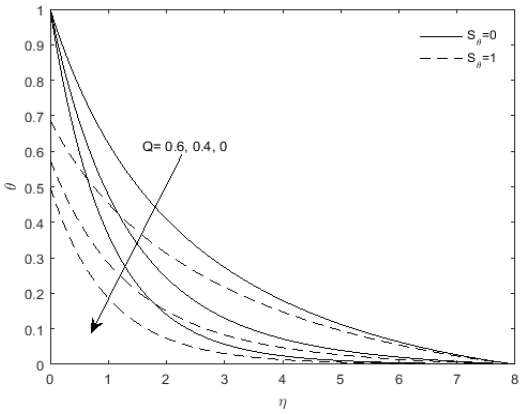

Figure 7. Temperature profile for Q

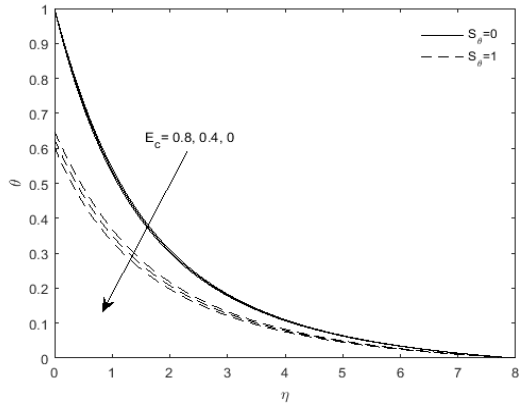

Figure 6. Temperature profile for E_c

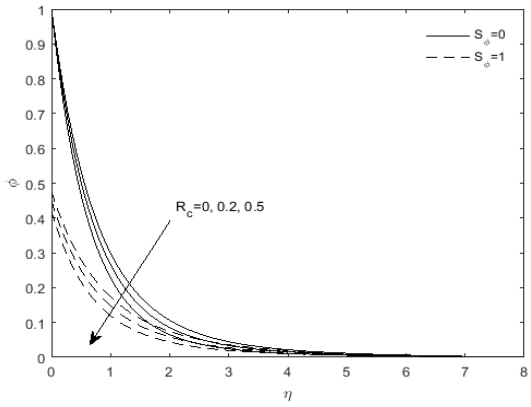

Figure 8. Concentration profile for R_c

Table 4 represents the effects of λ_1, λ_2, K_p, E_c, Q, R_c and S_c on skin friction, Nusselt number and Sherwood number. The other parameters are taken as $Pr = 1$, $S_f = 0.2$, $\delta = M = 0.5$, $R = S_\theta = S_\phi = S_r = 0.5$, $f_w = 0.2$. It is observed that increasing λ_1, λ_2 and K_p simultaneously increases skin friction coefficient and improves the rates of heat and mass transfer. This result shows a good agreement with the results of Mabood and Shateyi (2019). Further, it is noticed that higher values of E_c and Q help increase the skin friction but a reverse trend is shown in case of R_c and S_c.

Now higher values of E_c give a small temperature difference and so the rate of heat transfer decreases. Similarly, more the heat source parameter, Q less the rate of heat transfer. Likewise, increase in R_c and S_c leads to the heat transfer rate. Finally, the rate of mass transfer is analyzed. It is noted that all the parameters are directly proportional to the rate of mass transfer.

Table 4. The effects of λ_1, λ_2, K_p, E_c, Q, R_c and S_c on skin friction, Nusselt number and Sherwood number

λ_1	λ_2	K_P	E_C	Q	R_C	S_C	$f''(0)$	$-\theta'(0)$	$-\phi'(0)$
0	0.4	1	0.2	0.5	0.5	1	-1.21798	0.54844	0.81276
0.4	0.4	1	0.2	0.5	0.5	1	-1.12895	0.56331	0.81691
0.8	0.4	1	0.2	0.5	0.5	1	-1.04472	0.57564	0.82079
0.4	1	1	0.2	0.5	0.5	1	-1.04357	0.57352	0.82050
0.4	1.5	1	0.2	0.5	0.5	1	-0.97404	0.58120	0.82341
0.4	0.4	5	0.2	0.5	0.5	1	-0.96427	0.60003	0.81996
0.4	0.4	10	0.2	0.5	0.5	1	-0.94059	0.60559	0.82040
0.4	0.4	1	0.3	0.5	0.5	1	-1.12704	0.54000	0.82336
0.4	0.4	1	0.4	0.5	0.5	1	-1.12514	0.51675	0.82978
0.4	0.4	1	0.2	1	0.5	1	-1.09941	0.36564	0.84726
0.4	0.4	1	0.2	1.5	0.5	1	-0.94533	-0.53122	0.93526
0.4	0.4	1	0.2	0.5	1	1	-1.13499	0.56215	0.87529
0.4	0.4	1	0.2	0.5	2	1	-1.14328	0.56068	0.96254
0.4	0.4	1	0.2	0.5	0.5	2	-1.14444	0.56076	0.99120
0.4	0.4	1	0.2	0.5	0.5	10	-1.16627	0.55831	1.36828

6. Conclusions

The present study reveals the chemical reactive and dissipative MHD flow over a permeable stretching sheet embedded in a porous medium in the presence of heat source. The governing equations are solved using similarity transformation and Runge-Kutta method of fourth order along with shooting technique. The results are analyzed through graphs and tables. Some of the conclusions drawn from the results are as follows:

- Higher values of heat source parameter enhance the velocity.
- Porosity parameter contributes to the velocity of fluid.
- Fluid moves with higher velocity for higher values of viscous dissipation parameter.
- Higher values of chemical reaction parameter reduce the velocity of the fluid flow.
- Increasing values of dissipative heat represented by Ec, because of viscous dissipation gives rise to significant increase in temperature.
- Increase in porosity helps decrease the temperature significantly with and without thermal slip.
- Larger values of chemical reaction parameter lead to lower concentration. Higher values of E_c and Q lead to increase the skin friction but reverse trend is shown in case of R_c and S_c.

The limitations of the present study are:

(i) the Joulean dissipation, which is generated because of outward magnetic field interacting with conducting liquid, has been neglected.

(ii) induced magnetic field and Hall current are neglected, which should be studied in case of a high applied magnetic field strength.

The above limitations may be studied and considered as future directions for research. Effect of second slip conditions may also be taken care of and flow may be considered over different types of surfaces like a wavy surface.

Nomenclature

a	Stretching rate
D_T	Thermal diffusivity
B_0	Magnetic field of constant strength
E_c	Eckert number
C	Concentration of the fluid
f_w	Suction/injection
C_f	Local skin friction coefficient
k^*	Mean absorption coefficient
Cfr	Reduced skin friction
K_p	Porosity parameter
C_p	Specific heat
M	Magnetic field parameter
C_o	Reference concentration
Nur	Reduced Nusselt Number
C_w	Stretching sheet concentration
P_r	Prandtl number
C_∞	Ambient concentration
Q	Heat source parameter
D_d	Darcy dissipation parameter
R_c	Chemical reaction parameter
D_M	Molecular diffusivity
Re_x	Local Reynolds number
S_c	Schmidt number
ϕ	Nondimensional concentration
S_f	Velocity slip
η	Similarity variable
Shr	Reduced Sherwood number
ν	Kinematic viscosity
S_r	Soret number
α	Thermal diffusivity
S_θ	Thermal slip
β_c	Concentration expansion coefficient
S_ϕ	Solutal slip
β_T	Thermal expansion coefficient
T	Temperature
τ	Stress tensor
T_w	Stretching sheet temperature
δ	Unsteady parameter
T_0	Reference temperature
λ	Constant
T_∞	Ambient temperature
ρ	Density
u	x component of velocity
λ_1	Thermal buoyancy parameter
v	y component of velocity
λ_2	Solutal buoyancy parameter
x, y	Coorinates
σ^*	Stefan-Boltzmann constant

Greek Symbol

θ	Non-dimensional temperature

References

Ahmed, S. (2014). Numerical analysis for magneto hydro dynamic chemically reacting and radiating fluid past a non-isothermal impulsively started vertical surface adjacent to a porous regime. *Ain Shams Engineering Journal, 5*, 923-933.

Ahmed, S. & Kalita, K. (2014). Unsteady MHD chemically reacting fluid through a porous medium bounded by a non-isothermal impulsively-started vertical plate: A numerical technique. *Journal of Naval Architecture and Marine Engineering, 11*, 39-54.

Akbar, N. S. & Khan, Z. H. (2014). Heat transfer analysis of the peristaltic instinct of biviscosity fluid with the impact of thermal and velocity slips. *International Communications in Heat and Mass Transfer, 58*, 193- 199.

Ali, M. E. (1994). Heat transfer characteristics of a continuous stretching surface. *Warme-und Stoffubertragung, 29*, 227-234.

Anjali Devi, S. P. & Ganga, B. (2010). Dissipation effects on MHD nonlinear flow and heat transfer past a porous surface with prescribed heat flux. *Journal of Applied Fluid Mechanics, 3*, 1-6.

Baehr, H. D. & Stephan, K. (2006). *Heat and mass transfer* (2nd ed.). Berlin, Germany: Springer.

Biswal, M. M., Swain, B. K., Das, M., & Dash, G. C. (2022), Heat and mass transfer in MHD stagnation point flow towards an inclined stretching sheet embedded in a porous medium. *Heat Transfer, 51*, 4837-4857.

Chamber, P. L. & Young, J. D. (1958). The effects of homogeneous 1st order chemical reactions in the neighbourhood of a flat plate for destructive and generative reactions. *Physics of Fluids, 1*, 48-54.

Chamkha, A. J., Aly, A. M., & Mansour, M. A. (2010). Similarity solution for unsteady heat and mass transfer from a stretching surface embedded in a porous medium with suction/injection and chemical reaction effects. *Chemical Engineering Communications, 197*, 846-858.

Ferdows, M., Chapal, S. M., & Afify, A.A. (2014). Boundary layer flow and heat transfer of a nanofluid over a permeable unsteady stretching sheet with viscous dissipation. *Journal of Engineering Thermophysics, 23*, 216-228.

Gad-el-Hak (1999). The fluid mechanics of micro devices - the freeman scholar lecture, ASME. *Journal of Fluids Engineering, 121*, 5-33.

Hayat, T., Awais, M., & Hendi, A.A. (2012). Three-dimensional rotating flow between two porous wall with slip and heat transfer. *International Communications in Heat and Mass Transfer, 39*, 551-555.

Hunegnaw, D. & Kishan, N. (2017). Unsteady MHD heat and mass transfer flow over stretching sheet in porous medium with variable properties considering viscous dissipation and chemical reaction. *American Chemical Science Journal, 4*, 901-917.

Mabood, F. & Das, K. (2016). Melting heat transfer on hydromagnetic flow of a nanofluid over a stretching sheet with radiation and second-order slip. *The European Physical Journal Plus, 131*, 1-12.

Mabood, M. & Shateyi, S. (2019). Multiple slip effects on MHD unsteady flow heat and mass transfer impinging on permeable stretching sheet with radiation. *Modelling and Simulation in Engineering, 2019*, 1-11.

Makinde, O. D., Khan, W. A., & Khan, Z. H. (2016). Analysis of MHD nanofluid flow over a convectively heated permeable vertical plate embedded in a porous medium. *Journal of Nanofluids 5*, 574-580.

Makinde, O. D., Khan, Z. H., Ahmad, R., & Khan, W. A. (2018). Numerical study of unsteady hydromagnetic radiating fluid flow past a slippery stretching sheet embedded in a porous medium. *Physics of Fluids, 30*, 083601-083607.

Misra, J. C. & Sinha, A. (2013). Effect of thermal radiation on MHD flow of blood and heat transfer in a permeable capillary in stretching motion. *Heat Mass Transfer, 49*, 617-628.

Muthucumaraswamy, R. & Janakiramana, B. (2008). Mass transfer effect on isothermal vertical oscillating plate in presence of chemical reaction. *International Journal of Applied Mathematics and Mechanics, 4*, 66-74.

Mutuku-Njane, W. N. & Makinde, O. D. (2013). Combined effect of buoyancy force and Navier Slip on MHD flow of a nanofluid over a convectively heated vertical porous plate. *The Scientific World Journal, 2013*, 1-8.

Parida, B. C., Swain, B. K., & Senapati, N. (2021). Mass transfer effect on viscous dissipative MHD flow of nanofluid over a stretching sheet embedded in a porous medium. *Journal of Naval Architecture and Marine Engineering, 18*, 73-82.

Raza, J., Rohni, A.M., Omar, Z., & Awais, M. (2016). Heat and mass transfer analysis of MHD nanofluid in a rotating channel with slip effects. *Journal of Molecular Liquids, 219*, 703-708.

Reddy, M. G. (2016). Heat and mass transfer on Magnetohydrodynamic peristaltic flow in a porous medium with partial slip. *Alexandria Engineering Journal, 55*, 1225-1234.

Sekhar, K. R., Reddy, G. V., Raju, C. S. K., Ibrahim, S.M. & Makinde, O.D. (2018). Multiple slip effects on magnetohydrodynamic boundary layer flow over a stretching sheet embedded in a porous medium with radiation and joule heating. *Special Topics and Reviews in Porous Media*: *An International Journal, 9*, 117-132.

Swain, B. K. (2021). Effect of second order chemical reaction on MHD free convective radiating flow over an impulsively started vertical plate. *Journal of Nonlinear Modelling and Analysis, 3*, 167-178.

Swain, B. K., Biswal, M. M., & Dash, G. C. (2021). Effect of the second-order slip and heat source on dissipative MHD flow of blood through a permeable capillary in stretching motion. *International Journal of Ambient Energy*. doi:10.1080/01430750.2021.1979649.

Swain, B. K., Parida, B. C., Kar, S., & Senapati, N. (2020). Viscous dissipation and joule heating effect on MHD flow and heat transfer past a stretching sheet embedded in a porous medium. *Heliyon, 6*, 1-8. Retrieved from https://doi.org/10.1016/j.heliyon.2020.e05338

Swain, B. K. & Senapati, N. (2015). The effect of mass transfer on MHD free convective radiating flow over an impulsively started vertical plate embedded in a porous medium. *Journal of Applied Analysis and Computation, 5*, 18-27.

Swain, B. K., Senapati, N., & Dash, M. (2014). The effect of chemical reaction and thermal radiation on the hydromagnetic free convective rotating flow past an accelerated vertical plate in the presence variable heat and mass diffusion. *Der Chemica Sinica, 5*, 56-66.

Swain, B. K., Senapati, N., & Dash, M. (2017). Chemical reaction effect on MHD convective flow with heat and mass transfer past a semi-infinite vertical porous plate. *Journal of Advanced Mathematics and Applications, 6*, 1-8.

Turkyilmazoglu, M. (2013). Heat and mass transfer of MHD second order slip flow. *Computers and Fluids, 71*, 426-434.

Uddin, M. S. (2015).Viscous and joules dissipation on MHD flow past a stretching porous surface embedded in a porous medium. *Journal of Applied Mathematics and Physics, 3*, 1710-1725.

Venkateswarlu, B., Satya Narayana, P. V., & Tarakaramu, N. (2018). Melting and viscous dissipation effects on MHD flow over a moving surface with constant heat source. *Transactions of A. Razmadze Mathematical Institute, 172*, 618-630.